Synthesis by carbonate aminolysis and chiral recognition ability of cellulose 2,3-bis(3,5-dimethylphenyl carbamate)-6-(α-phenylethyl carbamate) selectors

Bui, CV; Rosenau, T; Hettegger, H

Published in:
Cellulose

DOI:
10.1007/s10570-022-04898-8

Published: 01/01/2023

Document Version
Final published version

Cellulose (2023) 30:153–168
https://doi.org/10.1007/s10570-022-04898-8

ORIGINAL RESEARCH

Synthesis by carbonate aminolysis and chiral recognition ability of cellulose 2,3-*bis*(3,5-dimethylphenyl carbamate)-6-(*α*-phenylethyl carbamate) selectors

Cuong Viet Bui · Thomas Rosenau · Hubert Hettegger

Received: 15 July 2022 / Accepted: 13 October 2022 / Published online: 25 October 2022

Abstract Novel chiral selectors based on cellulose 2,3-*bis*(3,5-dimethylphenyl carbamate)-6-(*α*-phenylethyl carbamate) were regioselectively synthesized by carbonate aminolysis and isocyanate chemistry. By oxycarbonylation with phenyl chloroformate, carbamoylation with 3,5-dimethylphenyl isocyanate, and subsequent aminolysis of the previously introduced reactive carbonate moiety at C6 with enantiopure (*R*)-or (*S*)-*α*-phenylethylamine, chiral selectors have been obtained, which regioselectively carry two different phenyl carbamate substituents. The cellulose derivatives were comprehensively characterized by ATR-FTIR, solid-state NMR, GPC, and elemental analysis. In parallel, 3-aminopropyl-functionalized silica gel as an inert carrier material for the chiral selectors was prepared and the obtained coated-type chiral stationary phases were characterized by both solid-state ^{29}Si NMR, ^{13}C NMR, and elemental analysis. The enantioseparation performance of the chiral selectors was studied and compared to cellulose *tris*(3,5-dimethylphenyl carbamate) as a reference. With this protocol in hand, certain shortcomings of conventional approaches towards the regioselective synthesis of polysaccharide-based chiral selectors were overcome, such as the limitation to standard isocyanate reagents, being able to apply now the whole wealth of commercially available (chiral) primary and also secondary alkylamines instead.

Supplementary Information The online version contains supplementary material available at https://doi.org/10.1007/s10570-022-04898-8.

C. V. Bui · T. Rosenau · H. Hettegger (✉)
Department of Chemistry, Institute of Chemistry of Renewable Resources, University of Natural Resources and Life Sciences, Vienna (BOKU), Konrad-Lorenz-Straße 24, 3430 Tulln, Austria
e-mail: hubert.hettegger@boku.ac.at

C. V. Bui
Department of Food Technology, Faculty of Chemical Engineering, University of Science and Technology, The University of Danang, 550000 Danang City, Vietnam

T. Rosenau
Faculty of Science and Engineering, Laboratory of Natural Materials Technology, Åbo Akademi University, Porthansgatan 3, 20500 Turku, Finland

Graphical abstract

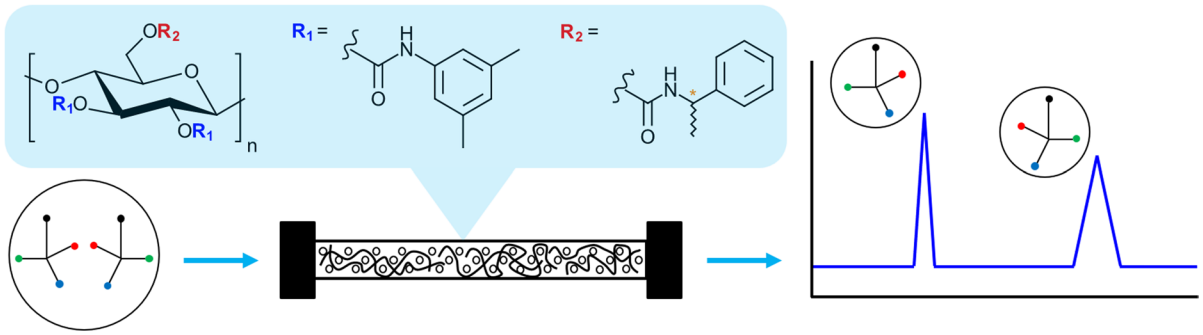

Keywords Aminolysis · Cellulose carbamate · Chiral stationary phase · Enantioseparation · High-performance liquid chromatography

Introduction

The chemistry of living matter is well defined by asymmetric characteristics of naturally occurring organic compounds, i.e., the presence of stereoisomers/enantiomers which exhibit different properties in chiral biological/biochemical systems (Pasteur 1858; Berthod 2006). In 1848, Louis Pasteur mechanically separated tartrate enantiomers under a microscope, which eventually led to the development of the concept of chirality (Pasteur 1858; D'Orazio 2020). However, the separation of enantiomers is rarely possible by mechanical means. Nowadays, mostly chiral stationary phases in high-performance liquid chromatography (HPLC) are used for the direct separation of pairs of enantiomers and other stereoisomers – both on an analytical and a preparative scale (Ahuja 1997; Subramanian 2008). Another separation approach is the use of chiral (enantiopure) mobile phase additives for the formation of transient diastereomeric species in HPLC – besides other indirect approaches, such as derivatization with chiral species and subsequent separation of the resulting diastereomers (Peng et al. 2016; Yu et al. 2019; Ao et al. 2022; Chen et al. 2022; Bao et al. 2022). Chiral/asymmetric synthesis (Xue et al. 2018; Wojaczyńska and Wojaczyński 2020; Qian et al. 2021; Zhu et al. 2021; Sun et al. 2022) and the kinetic resolution of enantiomers (Musa 2020; Spelmezan et al. 2020; Harwood et al. 2021; Huang et al. 2022; Yang et al. 2022), e.g., by enzymes, as approaches to obtain enantiopure compounds or at least non-racemic mixtures are to be mentioned as well.

The trailblazer for the direct enantioseparation with chiral selectors (CSs) based on cellulose derivatives was *inter alia* the work by Hesse and Hagel (1973) who applied cellulose triacetate as a CS in chromatography (Hesse and Hagel 1973). Since then, the importance of enantioseparation has been constantly increasing: in stereoselective synthesis (D'Orazio 2020), the analysis of enantiomers in food products (Rocco et al. 2013; Fanali et al. 2019; Alvarez-Rivera et al. 2020), insecticides (Zhao et al. 2019), pesticides (Carrão et al. 2019), herbicides (Martín-Biosca et al. 2001; Lao and Gan 2006; Jin et al. 2010), fungicides (Ying et al. 2009), and in pharmaceutical products (Mukherjee and Bera 2012; Singh et al. 2020) due to the different properties of enantiomers in biological systems (Tang et al. 2011; Yin et al. 2019a).

A series of homo-substituted cellulose and amylose derivatives carrying phenyl carbamate and/or benzoate moieties has been mainly developed by the Y. Okamoto, B. Chankvetadze, and E. Francotte research groups, and the respective CSPs were shown to possess a very high chiral discrimination capacity (Okamoto et al. 1986; Okamoto and Kaida 1994; Minguillón et al. 1996; Tang et al. 2010; Fanali et al. 2019) and to separate up to 90% of all tested

racemic compounds or enantiomeric mixtures (Ikai and Okamoto 2009; Shen and Okamoto 2016; Yin et al. 2019a).

In some cases, hetero-substituted cellulose derivatives were shown to have an even higher chiral separation performance in comparison to the respective homo-substituted derivatives (Acemoglu et al. 1998; Felix 2001; Katoh et al. 2011; Yin et al. 2019b). In 1993, Kaida and Okamoto pioneered the regioselective synthesis of hetero-substituted cellulose-type CSs, i.e., derivatives with more than one type of substituents, using sequential tritylation of C6–OH in cellulose and amylose followed by carbamoylation at C2–OH and C3–OH with isocyanates and subsequent deprotection (detritylation) (Kaida and Okamoto 1993). Various CSs based on cellulose derivatives with different phenyl carbamate and/or benzoate substituents have been reported since then (e.g., (Chassaing et al. 1996; Zheng et al. 2009; Shen et al. 2018). Several studies highlighted that the substituent at C6 of the AGU of the polysaccharide backbone had a significant influence on chiral recognition (Kaida and Okamoto 1993; Chassaing et al. 1996; Acemoglu et al. 1998; Felix 2001). The synthesis pathways towards these hetero-substituted cellulose CSs are typically rather laborious, chemical- and time-consuming, and they involve protecting group chemistry in combination with reactive isocyanate reagents. Chassaing et al. 1997 reported that in the case of hetero-substituted celluloses a chiral phenyl carbamate at C6 besides achiral phenyl carbamates at C2 and C3 had better enantioseparation than the counterpart homo-substituted with phenyl carbamates (Chassaing et al. 1997).

Besides the chemical structure of the CS, the enantioseparation performance of a coated chiral stationary phase is significantly dependent on the polysaccharide raw material, its molecular weight (Ichida et al. 1984; Chassaing et al. 1997; Okada et al. 2016; Zhang et al. 2020), the coating amount, the coating procedure and solvent used (Yashima et al. 1996; Wei et al. 2019), as well as silica gel characteristics, such as particle size, dispersity, or pore size (Yashima et al. 1996; Qin et al. 2010; Bezhitashvili et al. 2017; Kohout et al. 2019), and of course the respective analytes, the mobile phase and HPLC conditions (Yashima et al. 1996; Bui et al. 2021). To ensure an objective comparison and proper evaluation of the enantioseparation performance of novel CSs, all parameters except the actual chemical structures of these CSs should of course be kept constant.

Cellulose carbonates are a convenient platform for synthesizing cellulose derivatives, which is especially true for cellulose carbamate synthesis *via* aminolysis of the carbonates with simple primary and secondary alkyl amines (Pourjavadi et al. 2011; Elschner et al. 2013; Ganske and Heinze 2018). Cellulose aryl carbonates were shown to be more reactive than alkyl carbonates (Elschner and Heinze 2015). For details on carbonate aminolysis to obtain cellulose carbamates see the comprehensive studies by T. Heinze and others (Pourjavadi et al. 2011; Elschner et al. 2013; Elschner and Heinze 2015; Ganske and Heinze 2018). Different phenyl chloroformates have *inter alia* been evaluated as reagents for cellulose aryl carbonate synthesis and it was reported that most phenyl chloroformates react regioselectively (but not regiospecifically) with C6–OH, rather than with C2–OH and C3–OH groups of cellulose (Elschner et al. 2014; Ganske and Heinze 2018).

To the best of our knowledge, a compatible combination of isocyanate chemistry and oxycarbonylation/aminolysis has not yet been reported for the synthesis of hetero-substituted cellulose CSs. In this study, we present a sequence consisting of regioselective oxycarbonylation reaction with phenyl chloroformate at C6–OH, subsequent quantitative carbamoylation of C2–OH and C3–OH by isocyanates, and aminolysis of the reactive carbonate moieties, for the controlled synthesis of CSs bearing different substituents. The reactive carbonate moieties in this case are acting both as protecting group and reactive moiety for carbamate synthesis *via* aminolysis. The synthesis conditions for all steps were comprehensively optimized. The chemical structures of the cellulose derivatives, intermediates, and the target CSs were analyzed by FTIR, solid-state ^{13}C CP/MAS NMR, GPC, and elemental analysis (EA). In parallel, 3-aminopropyl-functionalized silica gel as a carrier for the CSs was prepared from silica and trialkoxysilane precursors and characterized by both solid-state ^{29}Si CP/MAS and ^{13}C CP/MAS NMR as well as EA.

The enantioseparation performance of the CSs was evaluated by HPLC in comparison to two references, an *in-house* prepared CS and a commercially available chiral column, both being based on the common cellulose *tris*(3,5-dimethylphenyl carbamate) CS.

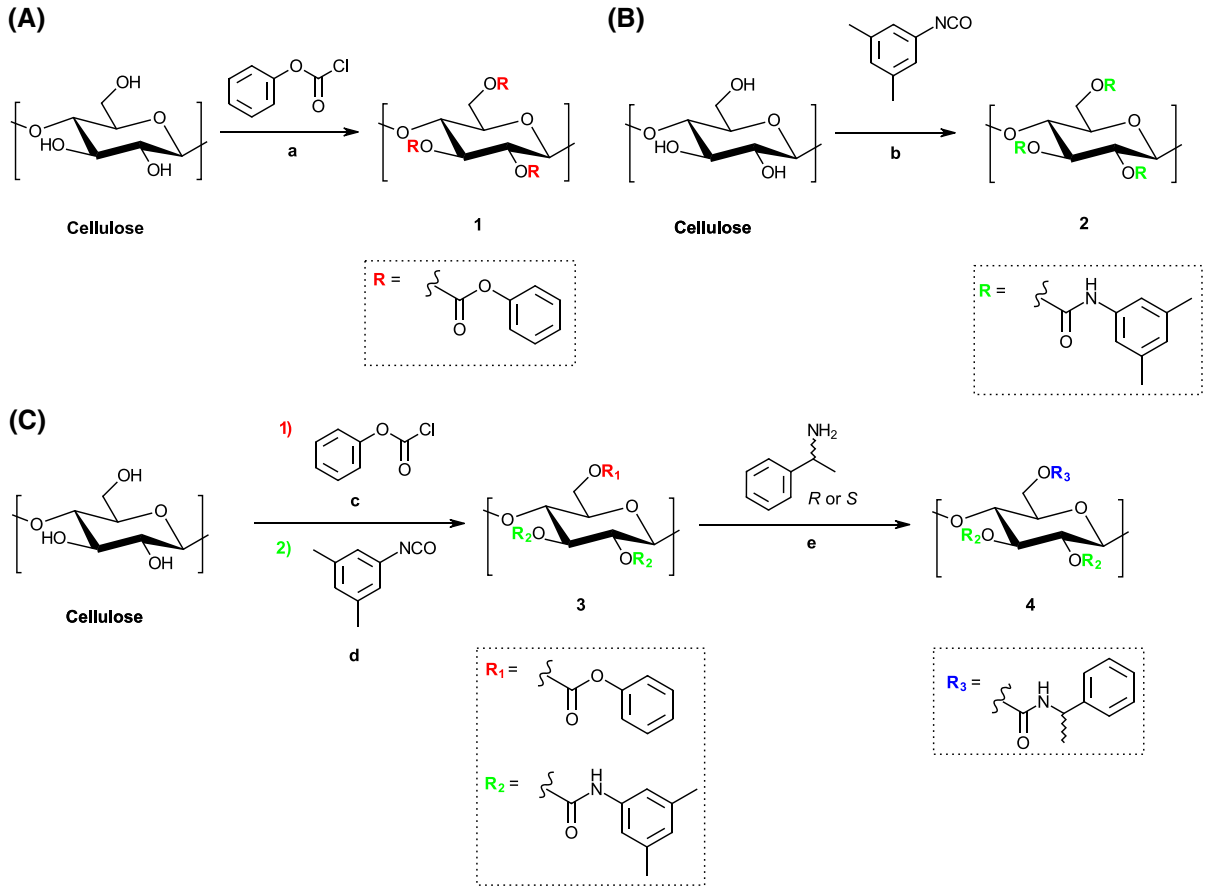

Fig. 1 **A** Chemical synthesis of the reference compound cellulose *tris*(phenyl carbonate) **1**; **B** synthesis of the reference chiral selector cellulose *tris*(3,5-dimethylphenyl carbamate) **2**; and **C** synthesis of the novel chiral selectors cellulose 2,3-*bis*(3,5-dimethylphenyl carbamate)-6-(*α*-phenylethyl carbamate) **4*R*** and **4*S***. Conditions: **a** DMAc/LiCl/pyridine, 0 °C, 12 h, N_2; **b** pyridine, 110 °C, 24 h, N_2; **c** DMAc/LiCl/pyridine, 0 °C, 12 h, N_2; **d** DMAc/LiCl/pyridine, 80 °C, 18 h, N_2; **e** DMF, 50 °C, 24 h, N_2

Results and discussion

Synthesis of the reference compound for structural comparison

Cellulose *tris*(phenyl carbonate) **1** (Fig. 1A) was synthesized as a reference compound for structural comparison to cellulose 2,3-*bis*(3,5-dimethylphenyl carbamate)-6-(phenyl carbonate) **3**, the latter being the precursor for the synthesis of the novel CSs **4*R*** and **4*S***. The reaction has been optimized towards an almost quantitative conversion of all hydroxy groups of the polysaccharide backbone.

The oxycarbonylation reaction was evaluated by ATR-FTIR and the chemical structure of cellulose derivative **1** was confirmed by solid-state ^{13}C NMR. Exemplary spectra are presented in Fig. S1 and Fig. S2, respectively (see Supplementary Information). The absence of IR bands from free OH groups at 3400 cm^{-1}, the presence of bands assigned to C=O at 1763 cm^{-1}, C=C aromatic rings at 1592, 1492, 1457, 835 cm^{-1}, as well as C-O at 1236 and 1205 cm^{-1} indicate that microcrystalline cellulose, the starting material used, was quantitatively oxycarbonylated. The FTIR spectrum of cellulose derivative **1** was fully consistent with literature data (Ganske and Heinze 2018). The solid-state ^{13}C CP/MAS NMR spectrum with carbon signals assigned to the C=O group at 152.9 ppm and the aromatic ring at 120.7, 126.1, 129.1, and 150.9 ppm confirmed this finding

Table 1 Elemental analysis results

Compound	Calculated (wt%)			Found (wt%, $n=3$)		
	C	**H**	**N**	**C**	**H**	**N**
2	65.66	6.18	6.96	64.60 ± 0.05	6.05 ± 0.08	6.81 ± 0.02
3	64.57	5.59	4.86	63.37 ± 0.55	5.59 ± 0.17	4.99 ± 0.08
4R	65.66	6.18	6.96	63.71 ± 0.12	5.99 ± 0.44	6.58 ± 0.07
4S	65.66	6.18	6.96	63.43 ± 0.09	5.31 ± 0.49	6.51 ± 0.07
APS	–	–	–	0.80 ± 0.01	0.14 ± 0.04	0.23 ± 0.00

Deviations from the calculated values are the result of incomplete substitution

(Fig. 2). The signal of the oxycarbonylated C6 was shifted downfield to 66.3 ppm.

Synthesis of the reference chiral selector

Cellulose *tris*(3,5-dimethylphenyl carbamate) was synthesized as a reference CS (Fig. 1B). This type of CS is a standard material in chiral separation columns and has been commercialized by several companies, e.g., Daicel Corp. and Phenomenex Inc. However, to compensate for differences in silica dimensions, cellulose starting material, column dimensions, coating procedure, and packing, we have decided to synthesize the reference CS in-house, allowing for a fairer comparison between the reference CS and novel synthesized CSs (***4R*** and ***4S***) since in this case all materials were processed in the same way. FTIR and solid-state ^{13}C NMR spectra of cellulose derivative **2** are shown in Fig. S3 and Fig. S4, and the related EA results are shown in Table 1, which also gives the values for the other cellulose derivatives synthesized.

The FTIR spectrum of cellulose derivative **2** shows bands related to N-H at 3320, C=O at 1722, aromatic C=C at 1615, 1539, 1455, 839, and C-O at 1213 cm^{-1}, and the absence of bands from free OH groups in cellulose around 3400 cm^{-1}, in agreement with literature data (Liu et al. 2013; Wei et al. 2019). The solid-state ^{13}C NMR showed resonances at 152.6 (C=O), 138.3, 125.0, 116.1 (aromatic ring), and 20.8 ppm (CH_3), confirming successful carbamoylation (Fig. S4). The chemical shift in solid-state ^{13}C NMR of the carbamoylated C6 was 64.9 ppm. The DS of the 3,5-dimethylphenyl carbamate moiety calculated based on the N content (EA) was 2.93 (98%). The molecular weight and dispersity of cellulose derivative **2** were 172.3 kDa (M_w) and 1.70 (Đ), respectively.

Synthesis of the precursor of the selectors

Oxycarbonylation with phenyl chloroformate at C6–OH, followed by carbamoylation with isocyanates

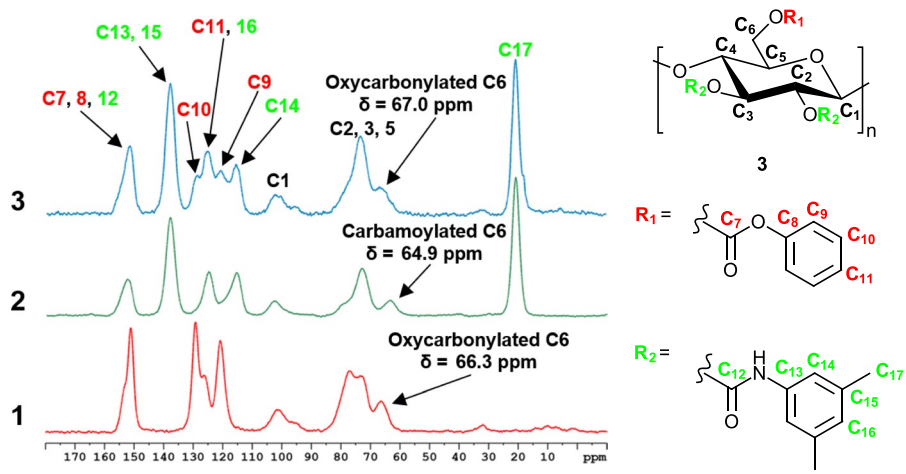

Fig. 2 Solid-state ^{13}C NMR spectra of the selectors' precursor **3** (blue) vs. the reference chiral selector **2** (green) and the model compound for structural comparison **1** (red)

at C2–OH and C3–OH, as a one-pot procedure, was used for the synthesis of compound **3** (Fig. 1C). Phenyl chloroformate was chosen due to higher reactivity in this case in comparison to *p*-nitrophenyl and 4-chlorophenyl chloroformates. The FTIR spectra of cellulose derivative **3** are shown in Fig. S5. The chemical structure of cellulose derivative **3** was additionally confirmed by solid-state ^{13}C NMR analysis in comparison to derivatives **1** and **2**. The respective spectra are shown in Fig. 2.

The absence of free OH groups (no bands around 3400 cm^{-1}), and bands for N-H at 3370 cm^{-1}, C=O at 1742 cm^{-1} (superposition of carbonate and carbamate carbonyls), C=C aromatic ring signals at 1612, 1543, 1453, 839 cm^{-1}, and C-O at 1207 cm^{-1} in the FTIR spectrum indicated that both oxycarbonylation and carbamoylation reactions proceeded successfully. The carbonyl signals of cellulose derivative **3** were at 1742 cm^{-1} in comparison to cellulose derivative **1** (1763 cm^{-1}) and cellulose derivative **2** (1722 cm^{-1}). The carbonate substituent, introduced first, remained stable during the subsequent carbamoylation reaction at elevated temperature (80 °C), which was also confirmed by solid-state ^{13}C NMR: the "marker" signals of C9 and C10 at 121.0 and 129.1 ppm, respectively, indicate the phenyl carbonate moieties on cellulose derivative **3**, while the signals of C13 and C15 at 138.0, C14 at 115.8 and C17 at 20.8 ppm confirm the presence of the 3,5-dimethylphenyl carbamate substituents. The C6 resonance at 67.0 ppm indicates that C6 is solely oxycarbonylated and not carbamoylated (see the downfield shift in comparison to compound **2** (64.9 ppm) in Fig. 2). The DS of the 3,5-dimethylphenyl carbamate based on the N content (EA) was calculated to be 2.05; the DS of phenyl carbonate was 0.93 (see Supplementary Information).

Synthesis of the novel chiral selectors by carbonate aminolysis

Oxycarbonylation at C6–OH, while having C2–OH and C3–OH carbamoylated, provides a "reactive protecting group" to be further modified by aminolysis. This converts the carbonate moiety into a carbamate. In this way, compound **3** was brought to reaction with two enantiopure alkyl amines: (*R*)- and (*S*)-*α*-phenylethyl amine. Virtually any primary or even secondary alkyl amine can be used in this way for obtaining carbamate structures, and the scope thus goes far beyond the relatively few functionalities that are accessible today by standard isocyanate reagents. It is important to point out that aromatic amines cannot be used for aminolysis of the carbonates due to their low nucleophilicity, which was already shown in a comprehensive study by (Elschner et al. 2013).

The FTIR spectra of cellulose derivatives ***4R*** and ***4S*** vs. **3** are shown in Fig. S6 and Fig. S7, respectively. The change of the carbonyl band from 1742 to approx. 1710 cm^{-1} (carbamate) and the significant decrease in the intensity of C-O signals at 1217 cm^{-1} indicate that the aminolysis reaction was successful. The solid-state ^{13}C NMR spectra of cellulose derivatives ***4R*** and ***4S*** vs. **3** are shown in Fig. 3 and Fig. S8. Characteristic resonances appear for C18 at approx. 51 ppm, C20 at 143 ppm, and C22 at 127 ppm. The chemical shift of C7 changes from 151.7 in

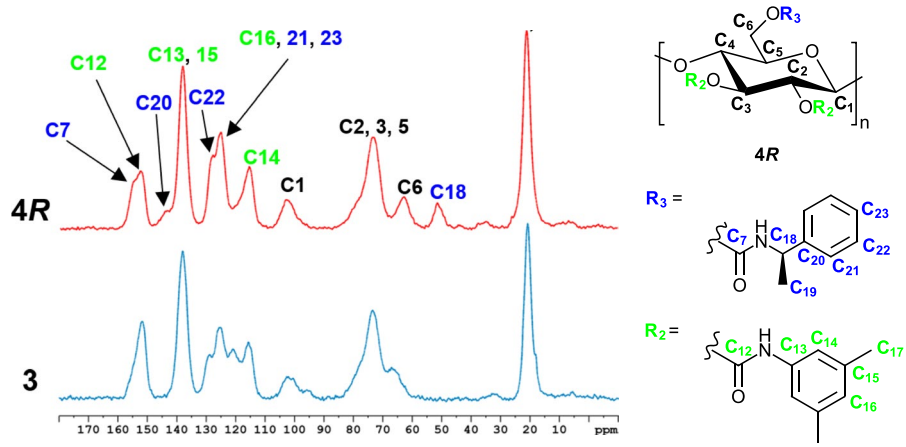

Fig. 3 Solid-state ^{13}C NMR spectra of cellulose derivatives ***4R*** (red) and the precursor **3** (blue)

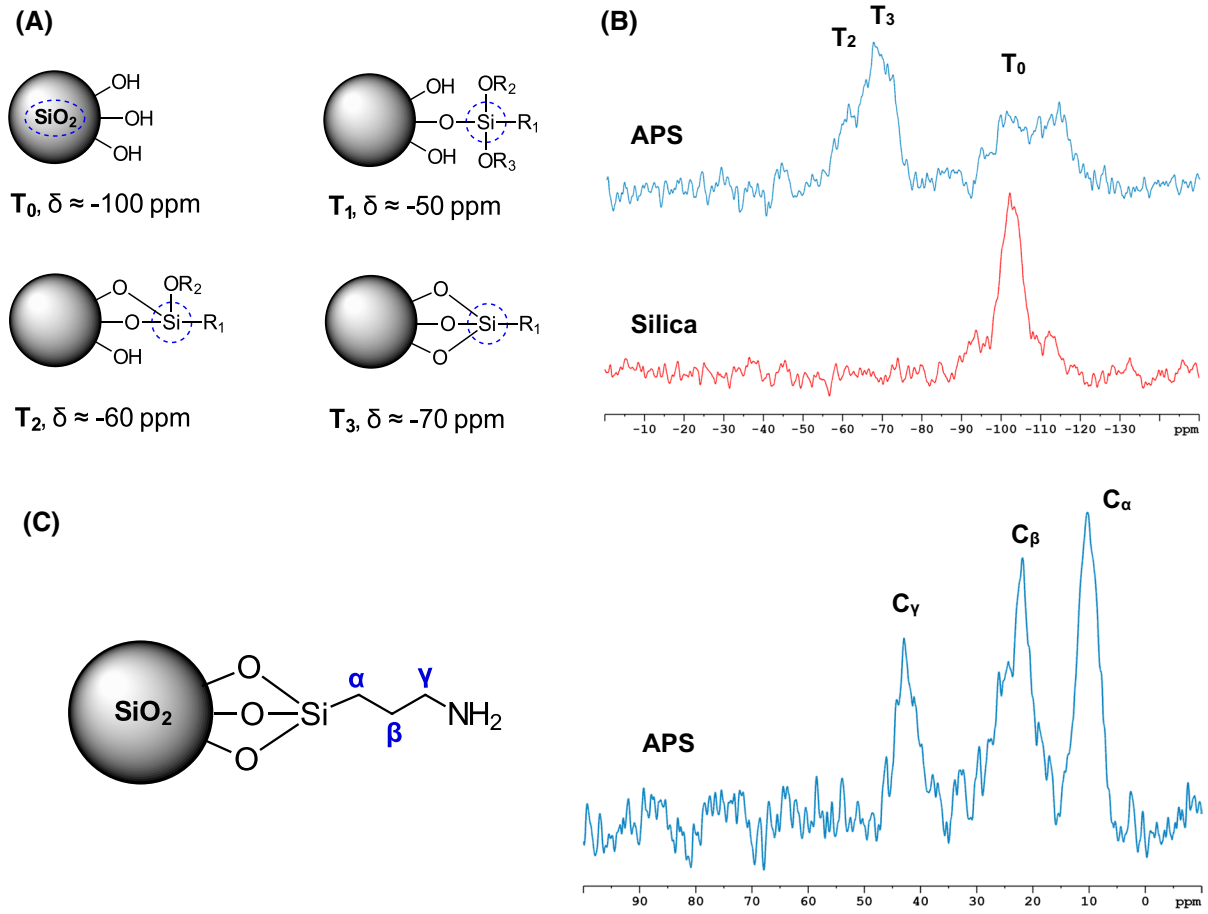

Fig. 4 **A** Alkoxysilane linkages to silica and respective shift values for the different species in solid-state ^{29}Si NMR; **B** Solid-state ^{29}Si CP/MAS NMR spectra of **APS** (blue) vs. non-modified silica gel (red); **C** The respective solid-state ^{13}C NMR spectrum of **APS**

the carbonate to 154 ppm in the carbamate substituent, as well as the shift of the C6 from 67 ppm in the carbonate to 63 ppm in the product. The absence of resonances of the phenyl carbonate moiety (C9 and C10, Fig. 3 and Fig. S8) confirmed that the aminolysis reactions proceeded nearly quantitatively. The degrees of substitution of the *R*- or *S*-*α*-phenylethyl carbamates, based on the N content from elemental analysis, were 0.78 and 0.75, respectively. The molecular weights and dispersities of the cellulose derivatives **4*R*** and **4*S*** were 238.8 and 234.2 kDa (M_w), and 3.53 and 2.76 (Đ), respectively.

Pre-functionalization of silica gel

The different silicon species and their resonances in solid-state ^{29}Si NMR adapted from (Salon et al. 2007) are presented in Fig. 4A. The solid-state ^{29}Si CP/MAS NMR spectra of **APS** vs. the non-modified silica gel starting material and the respective solid-state ^{13}C NMR spectrum of **APS** are shown in Fig. 4B C. The EA results for **APS** are shown in Table 1. The T_2 and T_3 resonances at approx. −60 and −70 ppm, respectively, in the solid-state ^{29}Si NMR spectrum of **APS** indicate successful covalent modification of the silica gel, as does the presence of ^{13}C resonances (solid-state NMR) (C_γ at approx. 42, C_β at approx. 22, and C_α at approx. 10 ppm). The loading of aminopropyl

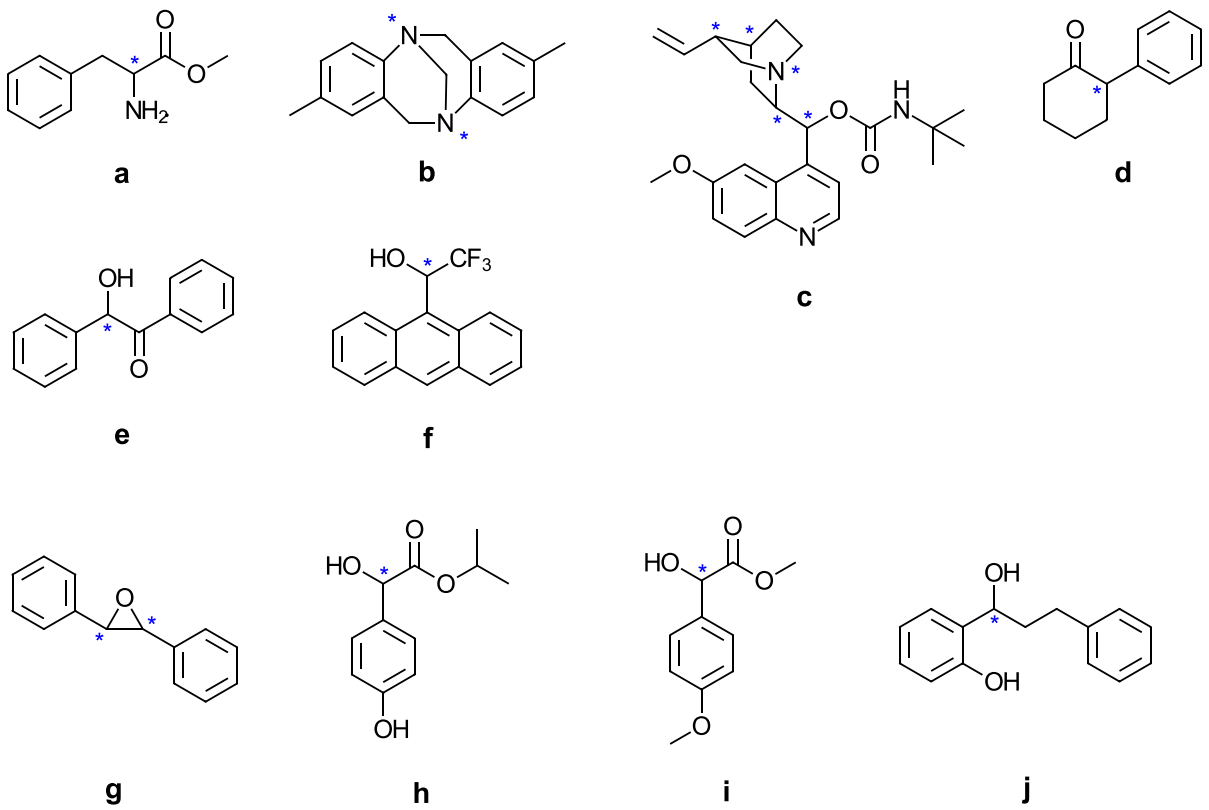

Fig. 5 The chemical structures of the chiral analytes **a–j**

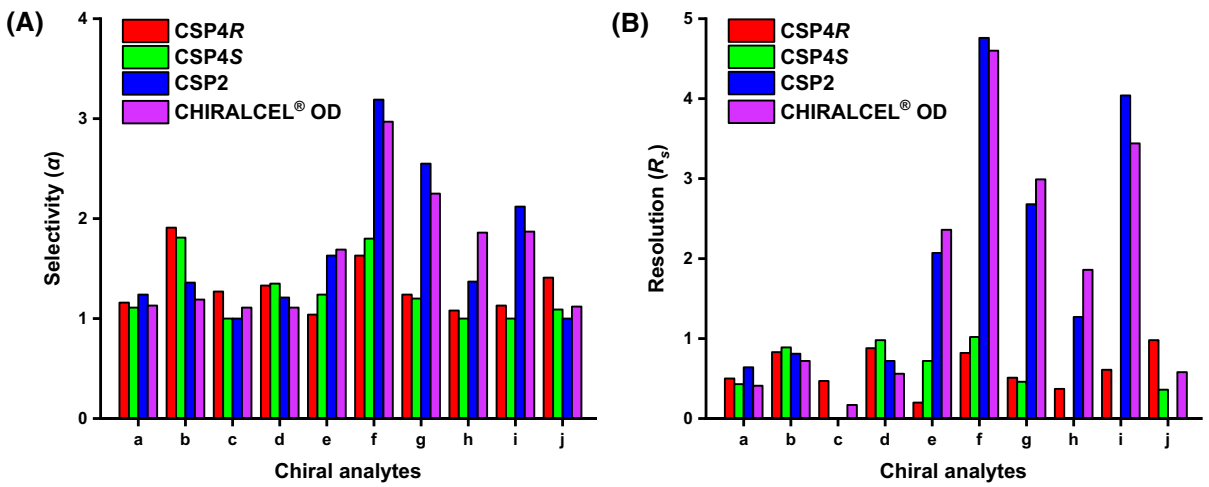

Fig. 6 **A** Selectivity (α) and **B** resolution (R_s) for the chiral analytes **a–j** on **CSP4*R*** and **CSP4*S*** in comparison to **CSP2** (*in-house* prepared reference) and commercially available CHIRALCEL® OD (same selector structure as **CSP2**)

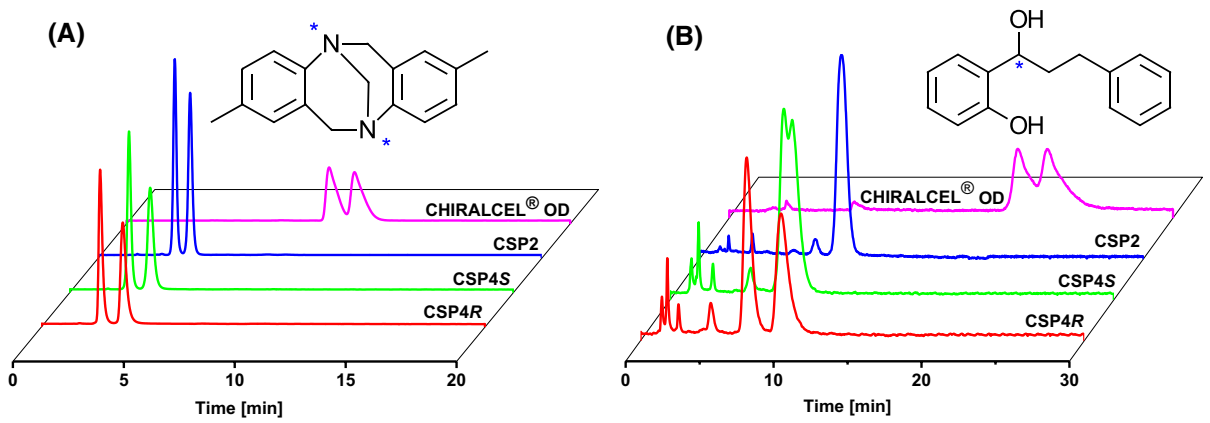

Fig. 7 HPLC chromatograms for **A** chiral analyte **b** and **B** compound **j**

groups, calculated based on the N content from elemental analysis, was 170 µmol/g (0.96 wt% N).

Evaluation of the enantioseparation performance

A series of ten chiral analytes (*α*-methyl-D,L-phenylalanine methyl ester **a**, Tröger's base **b**, a mixture of *pseudo*enantiomeric *tert*-butylcarbamoyl quinine and *tert*-butylcarbamoyl quinidine (ratio of 2:1, **c**), 2-phenylcyclohexanone **d**, benzoin **e**, Pirkle's alcohol **f**, *trans*-stilbene oxide **g**, mandelic acid isopropyl and methyl ester derivatives **h** and **i**, and 1-(*o*-hydroxyphenyl)-3-phenyl-1-propanol **j**, see Fig. 5) was used to study the enantioseparation performance of the developed column materials (**CSP4*R*** and **CSP4*S***) in comparison to an *in-house* reference column (**CSP2**) and a commercial reference column (CHIRALCEL® OD).

The chromatographic retention factor (k_1), selectivity (α), and resolution (R_s) data of the chiral analytes for all tested CSPs are summarized in Fig. 6 and Table S1. Example HPLC chromatograms for the chiral analytes **b** and **j** are shown in Fig. 7.

All of the selected chiral analytes could be – at least partially – separated on both the *in-house* prepared reference material **CSP2** and the commercially available CHIRALCEL® OD column. Especially, the chiral analytes **e**, **f**, **g**, and **i** with R_s values > 1.5 were baseline-separated, while the chiral analytes **a**, **b**, and **d** with $0 < R_s < 1.5$ were at least partly separated. The analytes **c** and **j** were partly separated on CHIRALCEL® OD with $R_s = 0.17$ and 0.58, respectively, but not separated on **CSP2**. Chiral analyte **h** was baseline separated on CHIRALCEL® OD with $R_s = 1.86$, but only partly on **CSP2** ($R_s = 1.27$). Analytes **a**, **b**, **d**, **f**, and **i** were better resolved on **CSP2**, analytes **e** and **g** on CHIRALCEL® OD. The highest selectivity and resolution among the tested chiral analytes on both **CSP2** and CHIRALCEL® OD was seen for analyte **f** ($\alpha = 3.19$ and 2.97, $R_s = 4.76$ and 4.60, respectively). Overall, the resolution values in the case of the reference **CSP2** were quite comparable to the commercial column CHIRALCEL® OD. The CHIRALCEL® OD column was added to this study as a commercially available benchmark column. Note some differences in silica gel dimensions (10 vs. 7 µm) and column dimensions (250×4.6 vs. 150×4 mm) for CHIRALCEL® OD and **CSP2**, respectively.

Regarding the enantioseparation performance of **CSP4*R*** and **CSP4*S***, the chiral analytes **a**, **b**, **d**, **e**, **f**, **g**, and **j** were partly separated on these columns with R_s values < 1.5. The analytes **b**, **d**, **e**, and **f** were better separated on **CSP4*S***, while analytes **a** and **j** had higher resolution on **CSP4*R***. The analytes **c**, **h**, and **i** were partly separated on **CSP4*R*** ($R_s = 0.47$, 0.37, and 0.61, respectively), but not on **CSP4*S***. The chiral analytes **b** and **d** gave higher resolution values on **CSP4*R*/CSP4*S*** than on the reference column **CSP2**, while **CSP2** showed higher enantioseparation for the chiral analytes **a**, **e**, **f**, and **g** (see Fig. 6 and Table S1). The chiral analytes **h** and **i** gave higher resolution values on **CSP2** compared to **CSP4*R***, while they could not be separated on **CSP4*S*** with the applied mobile

phase conditions. The analyte **j** was partly separated on both **CSP4*R*** and **CSP4*S*** with $R_s = 0.94$ and 0.36, respectively, however, it could not be separated on **CSP2**. Analyte **c** was partly separated on **CSP4*R*** ($R_s = 0.47$), but it could not be separated on both **CSP4*S*** and **CSP2**. It is noteworthy that the chiral analytes **c** and **j** had a higher resolution on **CSP4*R*** with $R_s = 0.47$ and 0.98 than on CHIRALCEL® OD with $R_s = 0.17$ and 0.58, and they could not be separated at all on **CSP2**.

Conclusion

Carbonate aminolysis and isocyanate chemistry were exploited to obtain novel cellulose 2,3-*bis*(3,5-dimethylphenyl carbamate)-6-(*α*-phenylethyl carbamate)-based CSs. The regioselective oxycarbonylation of C6–OH of the polysaccharide backbone of cellulose with phenyl chloroformate for obtaining a "reactive protecting group" for later aminolysis of the carbonate moieties was optimized. The hydroxy groups at C2 and C3 of the intermediate were subsequently carbamoylated with 3,5-dimethylphenyl isocyanate in the second step of this one-pot procedure, having a DS of 3,5-dimethylphenyl carbamate of 2.05 and a DS of the phenyl carbonate of 0.93. Aminolysis of the reactive carbonate moiety with two exemplary enantiopure amines – (*R*)- and (*S*)-*α*-phenylethyl amine – yielded novel hetero-substituted cellulose-based CSs. This protocol overcomes the limitations of conventional approaches to CSs, set by the limited variety of isocyanates available. With this protocol in hand, cellulose carbamates are accessible from simple alkyl amines, which offer much wider substrate choices, without the need to resort solely to isocyanate chemistry. Two enantiopure compounds have been used as exemplary amines. However, virtually any primary and also secondary alkyl amine could be used, and this wealth of options will be exploited in our future work to optimize enantioseparation. The obtained chiral selectors were coated onto silica and the obtained CSPs were compared to an *in-house* prepared reference material and a commercial column material. The newly developed CSPs have shown good overall separation performance, well comparable to the commercial references, although no clear trends can be identified at the moment. Some of the chiral analytes were even better separated on the novel CSPs than with the reference columns. We hope that with this work we have been able to demonstrate that the synthesis of regioselectively modified chiral selectors by oxycarbonylation and subsequent aminolysis is advantageously possible, that the resulting hetero-substituted cellulose derivatives can be used as CSs for enantioseparation in chiral HPLC, and that this approach is certainly worth further exploitation.

Materials and methods

Materials

Microcrystalline cellulose (Avicel® PH-101), *p*-cymene (99%), *α*-methyl-D,L-phenylalanine methyl ester (98%, **a**), Tröger's base (98%, **b**), and *trans*-stilbene oxide (98%, **g**) were purchased from Sigma-Aldrich (Schnelldorf, Germany). Microcrystalline cellulose was dried at 40 °C in a vacuum oven for at least two days before use. *Pseudo*enantiomeric *tert*-butylcarbamoyl quinine and *tert*-butylcarbamoyl quinidine **c** were kindly provided by Assoc.Prof. Dr. Michal Kohout (University of Chemistry and Technology, Prague, Czech Republic). 3,5-Dimethylphenyl isocyanate (> 98%), phenyl chloroformate (> 98%), (*R*)-(+)-*α*-phenylethyl amine (> 99%), (*S*)-(-)-*α*-phenylethyl amine (> 98%), 2-phenylcyclohexanone (> 98%, **d**), benzoin (> 98%, **e**) and Pirkle's alcohol (> 99%, **f**) were purchased from TCI Europe N.V. (Zwijndrecht, Belgium). The mandelic acid derivatives (**h** and **i**) and 1-(*o*-hydroxyphenyl)-3-phenyl-1-propanol **j** were synthesized *in-house* according to standard procedures. Silica gel (7 µm, 1000 Å) was purchased from Daisogel Osaka Soda Co., Ltd. (Japan). Empty stainless HPLC columns (150 × 4 mm, i.d.) and column hardware were purchased from Bischoff Analysentechnik u. -geräte GmbH (Leonberg, Germany). A commercial CHIRALCEL® OD column (10 µm silica gel, 250 × 4.6 mm, i.d.) from Daicel Chiral Technologies Europe SAS (Illkirch Cedex, France) was used for comparative purposes. The organic solvents such as *N*,*N*-dimethylacetamide (DMAc), *N*,*N*-dimethylformamide (DMF), toluene, and pyridine were all reagent grade and dried over 3 Å molecular sieves (Sigma-Aldrich, Schnelldorf,

Germany) for at least three days before use. Ethanol (EtOH) and methanol (MeOH) for precipitation and washing were of technical grade and obtained from Carl Roth GmbH + Co. KG (Karlsruhe, Germany) or Fisher Scientific (Vienna, Austria). The HPLC solvents *n*-hexane (95%) and 2-propanol (99.9%) were obtained from Fisher Scientific.

Instrumentation

ATR-FTIR spectra were recorded on a Frontier IR Single-Range spectrometer (PerkinElmer, Waltham, Massachusetts, US) equipped with a diamond/ZnSe crystal, $LiTaO_3$ detector, and KBr windows. FTIR spectra were evaluated using SpectraGryph software (version v1.2.15). Solid-state ^{13}C CP/MAS (12 kHz) and ^{29}Si CP/MAS (8 kHz) NMR experiments were carried out with an Avance III HD instrument (Bruker, Rheinstetten, Germany) with a resonance frequency of 100.67 MHz for ^{13}C and 79.53 MHz for ^{29}Si. Data processing was carried out with ACD/NMR Processor Academic Edition 12.01 and TopSpin 3.6.2 software (Bruker). Chemical shifts (δ) are given in ppm. Elemental analyses were carried out at the microanalytical laboratory of the University of Vienna with a EURO EA 3000 CHNS-O instrument (HEKAtech, Wegberg, Germany), and halide contents were determined by argentometry. GPC analyses were performed according to standard procedures (Jusner et al. 2022). An Agilent Technologies, Inc. (Santa Clara, CA, USA) 1100 HPLC apparatus equipped with a quaternary pump (G1311A), autosampler (G1313A), and DAD (G1315A) was used to evaluate the enantioseparation performance of the chiral columns. OpenLab CDS software (Agilent) was used for chromatography data processing and evaluation.

Synthesis

Synthesis of cellulose tris(phenyl carbonate) ***1***

Cellulose *tris*(phenyl carbonate) was synthesized according to a protocol by (Ganske and Heinze 2018) with modification. Microcrystalline cellulose (1.0 g) was immersed and vigorously stirred in anhydrous DMAc (30 mL) under a dry nitrogen atmosphere. The suspension was heated at 120 °C for 2 h. Anhydrous LiCl (1.8 g) was slowly added after cooling down to < 90 °C, and the mixture was continuously stirred at RT until a clear solution was formed. Anhydrous pyridine (3.0 mL) was slowly added to the solution, which was then cooled to 0 °C by an ice/water bath. Phenyl chloroformate (6 molar equivalents with respect to the AGU repeating unit of cellulose) was added dropwise to the solution and the mixture was allowed to stir for 12 h. The mixture was added to a large excess of distilled water (DW) for the precipitation of crude cellulose derivative **1**, which was then collected by vacuum filtration, washed with a large excess of DW and with EtOH (2 × each), and dried at 40 °C in a vacuum oven for two days. Crude cellulose derivative **1** was re-dissolved in acetone (250 mL) and residual LiCl was separated by vacuum filtration through a sintered frit. Acetone was evaporated for the most part by rotary evaporation under reduced pressure and cellulose derivative **1** was precipitated in EtOH, collected by vacuum filtration, washed with a large excess of EtOH and DW (2 × each), and dried at 40 °C in a vacuum oven for two days. Yield: 2.66 g, 83 wt%. Cellulose derivative **1** is soluble in DMAc, acetone, pyridine, DMF, and THF.

Synthesis of cellulose tris(3,5-dimethylphenyl carbamate) ***2***

Synthesis protocols based on (Okamoto et al. 1984) and (Miaomiao et al. 2017) were applied with modifications to synthesize cellulose *tris*(3,5-dimethylphenyl carbamate) as a reference CS. Microcrystalline cellulose (2.0 g) was immersed and vigorously stirred in anhydrous pyridine (40 mL) under a dry nitrogen atmosphere. 3,5-Dimethylphenyl isocyanate (6 molar equivalents with respect to the AGU repeating unit of cellulose) was added dropwise. The temperature of the suspension was increased to 110 °C and the carbamoylation reaction was continued for 24 h. A large excess of MeOH was used to precipitate crude cellulose derivative **2**, which was then collected by vacuum filtration, washed with MeOH and with DW (2 × each), and then dried in a vacuum oven at 40 °C for two days. Further purification of cellulose derivative **2** was performed by re-dissolution in pyridine and re-precipitation in MeOH, vacuum filtration, and washing of the precipitate with MeOH and with DW (2 × each). The purified cellulose derivative **2** was dried in a vacuum oven at 40 °C for two days. Yield: 5.73 g, 77 wt%. Cellulose derivative **2** is soluble in pyridine,

acetone, DMAc, DMF, and THF, but not in acetonitrile. Swelling was observed in $CHCl_3$.

One-pot two-step synthesis of cellulose 2,3-bis(3,5-dimethylphenyl carbamate)-6-(phenyl carbonate) ***3***

Microcrystalline cellulose (3.0 g) was immersed and vigorously stirred in anhydrous DMAc (90 mL) under a dry nitrogen atmosphere. The mixture was heated at 120 °C for 2 h. After cooling down to < 90 °C, anhydrous LiCl (5.4 g) was slowly added to the suspension and the mixture was continuously stirred at RT until a clear solution was formed. Anhydrous pyridine (9.0 mL) was then added to the solution, which was cooled down to 0 °C by an ice/water bath. Phenyl chloroformate (1.5 molar equivalents with respect to the AGU repeating unit of cellulose) was added dropwise. The oxycarbonylation reaction was carried out for 12 h. Then, anhydrous pyridine (30 mL) was added to the solution, which was heated to 80 °C, followed by the dropwise addition of 3,5-dimethylphenyl isocyanate (5 molar equivalents with respect to the AGU repeating unit of cellulose). The carbamoylation reaction was performed for 18 h at 80 °C. The solution was cooled down to RT and a large excess of DW was used to precipitate crude cellulose derivative **3**, which was collected by vacuum filtration, washed with a large excess of DW and with EtOH (2 × each), and dried at 40 °C in a vacuum oven for two days. Crude cellulose derivative **3** was re-dissolved in acetone (750 mL), and residual LiCl was separated by vacuum filtration through a sintered glass frit. Acetone was evaporated for the most part by rotary evaporation under reduced pressure and cellulose derivative **3** was re-precipitated in a large excess of EtOH, collected by vacuum filtration, washed with a large excess of EtOH and with DW (2 × each), and dried at 40 °C in a vacuum oven for two days. Yield: 9.76 g, 92 wt%. Cellulose derivative **3** is soluble in DMAc, pyridine, acetone, DMF, and THF.

Synthesis of cellulose 2,3-bis(3,5-dimethylphenyl carbamate)-6-((R/S)-α-phenylethyl carbamate) ***4R and 4S***

Cellulose derivative **3** (2.5 g) was stirred in anhydrous DMF (50 mL) under a dry nitrogen atmosphere until a clear solution was formed. Either (*R*)-(+)-α-methylbenzylamine or (*S*)-(-)-α-methylbenzylamine (5 molar equivalents with respect to the repeating unit of cellulose derivative **3**) was added dropwise, and the aminolysis reactions were performed at 50 °C for 24 h. After cooling down to RT, a large excess of EtOH was used to precipitate crude cellulose derivatives **4*R*** or **4*S***, which were then collected by vacuum filtration, and washed with a large excess of EtOH and DW (2 × each). Crude cellulose derivative **4*R*** or **4*S*** was re-dissolved in DMF, re-reprecipitated in a large excess of EtOH, collected by vacuum filtration, and washed with a large excess of EtOH and with DW (2 × each). Purified cellulose derivative **4*R*** or **4*S*** was dried at 40 °C in a vacuum oven for 2 days. Yield **4*R***: 2.37 g, 91 wt%; **4*S***: 2.42 g, 93 wt%. Cellulose derivatives **4*R*** and **4*S*** are soluble in pyridine, acetone, DMAc, DMF, and THF, but not in acetonitrile. Swelling was observed in $CHCl_3$.

Synthesis of 3-aminopropyl-functionalized silica gel ***(APS)***

The protocols reported by (Engelhardt and Orth 1987; Yashima et al. 1996; Okada et al. 2016) were adapted to synthesize 3-aminopropyl-functionalized silica gel (**APS**) as an inert carrier for the CSs. Silica gel (10 g) was immersed in toluene (200 mL), mechanically stirred, and the mixture was dried by azeotropic distillation in a dry nitrogen atmosphere. After distilling off about half of the volume of toluene, the temperature of the suspension was reduced to 80 °C, triethylamine (1 mL) was added as a catalyst, followed by the addition of (3-aminopropyl)triethoxysilane (10 mL). The reaction mixture was allowed to stir for 48 h. The suspension was then cooled down to RT and crude **APS** was collected by vacuum filtration through a sintered glass frit (DURAN®, porosity 4), washed with hot toluene (100 mL), EtOH (100 mL), and with DW (2 × 200 mL). **APS** was then dried at 40 °C in a vacuum oven for two days. Yield: 9.96 g.

CSP preparation and HPLC method

Silica coating

The coating amount of each CS on **APS** was 20 wt% (Zhang and Francotte 1995). The coating was performed in three steps for the most homogeneous possible distribution of the CS on **APS** (Wei et al. 2019).

CS (0.4 g) was dissolved in THF (40 mL) and the homogeneous solution was transferred to a round-bottomed flask that contained dry **APS** (3.2 g). THF was slowly evaporated at 40 °C at 357 mbar in a rotary evaporator. Then, a solution of CS (0.2 g) dissolved in THF (20 mL) was added to the round-bottomed flask, and the solvent was evaporated again. The coating process was repeated once more. After solvent evaporation and drying in a vacuum oven at 40 °C overnight, the coated silica particles were sieved through an analytical sieve before packing (40 µm mesh size).

Column packing

The coated and sieved silica particles (2.3 g) were suspended in a mixture of isopropanol (20 mL) and acetic acid (100 µL). The mixture was sonicated for 20 min to form a homogeneous slurry, which was then packed *in-house* under high pressure (max. 290 bar) into an empty stainless steel HPLC column. As a compacting agent, MeOH was used (app. 120 mL). After packing, the columns were rinsed with isopropanol until use.

HPLC method

The columns packed with **CSP2** (CS = cellulose derivative **2**), **CSP4*R*** (CS = **4*R***), and **CSP4*S*** (CS = **4*S***) were rinsed with *n*-hexane/isopropanol in a stepwise gradient (30:70, 60:40, 90:10, v/v) before use. The concentration of the analytes was 1 mg/mL each. The flow rate and injection volume were set to 1 mL/min and 5 µL, respectively. The absorbance of all analytes was recorded at 254 nm. *p*-Cymene was used to determine the dead time (t_0). All measurements were carried out in triplicate.

Acknowledgments The authors would like to thank the University of Natural Resources and Life Sciences, Vienna (BOKU) and the County of Lower Austria for their financial support in the framework of the "Austrian Biorefinery Center Tulln" (ABCT) and the BOKU doctoral school "Advanced Biorefineries: Chemistry & Materials" (ABC&M). C.V.B. is grateful for an Ernst Mach Grant (ASEA-UNINET, ICM-2019-13801). The financial support by the Gesellschaft für Forschungsförderung Niederösterreich m.b.H. (H.H., project LSC20-002) is gratefully acknowledged. Peter Frühauf (University of Vienna) is gratefully acknowledged for his support in column packing. Open access funding is provided by the University of Natural Resources and Life Sciences, Vienna (BOKU). Assoc. Prof. Dr. Michal Kohout (University of Chemistry and Technology, Prague, Czech Republic) is acknowledged for providing chiral analytes.

Author contributions C.V.B, T.R. and H.H. contributed to the study conception and design. Material preparation, data collection and analysis were performed by C.V.B. The original draft of the manuscript was written by C.V.B, including visualization. Review & editing by T.R. and H.H. Supervision, project administration and funding acquisition by T.R. and H.H. All authors commented on previous versions of the manuscript. All authors read and approved the final manuscript.

Funding Open access funding provided by University of Natural Resources and Life Sciences Vienna (BOKU). The authors would like to thank the University of Natural Resources and Life Sciences, Vienna (BOKU) and the County of Lower Austria for their financial support in the framework of the "Austrian Biorefinery Center Tulln" (ABCT) and the BOKU doctoral school "Advanced Biorefineries: Chemistry & Materials" (ABC&M). C.V.B. is grateful for an Ernst Mach Grant (ASEA-UNINET, ICM-2019-13801). The financial support by the Gesellschaft für Forschungsförderung Niederösterreich m.b.H. (H.H., project LSC20-002) is gratefully acknowledged. Open access funding is provided by the University of Natural Resources and Life Sciences, Vienna (BOKU).

Declarations

Conflict of interest The authors declare that they have no conflict of interest.

Consent for publication All authors agreed to the publication in the submitted form.

References

Acemoglu M, Küsters E, Baumann J, Hernandez I, Pong-Mak C (1998) Synthesis of regioselectively substituted cellulose derivatives and applications in chiral chromatography. Chirality 10(4):294–306

Ahuja S (1997) Chiral Separations and Technology: An Overview. In: Ahuja S (ed) Chiral separations: applications and technology. Amer Chemical Society, Washington DC

Alvarez-Rivera G, Bueno M, Ballesteros-Vivas D, Cifuentes A (2020) Chiral analysis in food science. Trends Analyt Chem 123:115761

Ao Q, Zhao H, Tong T, Peng Y, He Z (2022) Enantioseparation of basic drugs by reverse phase high-performance liquid chromatography system using carboxymethyl-β-cyclodextrin as chiral mobile phase additive. Chirality 34(8):1128–1139

Bao H, Sun W, Sun H, Jin Y, Gong X, Chu C, Tong S (2022) Liquid chromatographic study of two structural isomeric pentacyclic triterpenes on reversed-phase stationary phase with hydroxypropyl-β-cyclodextrin as mobile phase additive. J Pharm Biomed Anal 207:114420

Berthod A (2006) Chiral recognition mechanisms. Anal Chem 78 (7):2093–2099

Bezhitashvili L, Bardavelidze A, Ordjonikidze T, Chankvetadze L, Chity M, Farkas T, Chankvetadze B (2017) Effect of pore-size optimization on the performance of polysaccharide-based superficially porous chiral stationary phases for the separation of enantiomers in high-performance liquid chromatography. J Chromatogr A 1482:32–38

Bui CV, Rosenau T, Hettegger H (2021) Polysaccharide-and β-Cyclodextrin-based chiral selectors for enantiomer resolution: Recent developments and applications. Molecules 26(14):4322

Carrão DB, Perovani IS, de Albuquerque NCP, de Oliveira ARM (2019) Enantioseparation of pesticides: A critical review. Trends Analyt Chem 122:115719

Chassaing C, Thienpont A, Félix G (1996) Regioselective carbamoylated and benzoylated cellulose for the separation of enantiomers in high-performance liquid chromatography. J Chromatogr A 738(2):157–167

Chassaing C, Thienpont A, Soulard MH, Felix G (1997) Regioselectivity carbamoylated polysaccharides for the separation of enantiomers in high-performance liquid chromatography. J Chromatogr A 786(1):13–21

Chen B, You H, Fang L, Lin T, Xu P, Chu C, Tong S (2022) Enantioseparation of five racemic N-alkyl drugs by reverse phase HPLC using sulfobutylether-β-cyclodextrin as a chiral mobile phase additive. J Sep Sci 45(11):1847–1855

D'Orazio G (2020) Chiral analysis by nano-liquid chromatography. Trends Analyt Chem 125:115832

Elschner T, Heinze T (2015) Cellulose carbonates: a platform for promising biopolymer derivatives with multifunctional capabilities. Macromol Biosci 15(6):735–746

Elschner T, Ganske K, Heinze T (2013) Synthesis and aminolysis of polysaccharide carbonates. Cellulose 20(1):339–353

Elschner T, Kötteritzsch M, Heinze T (2014) Synthesis of cellulose tricarbonates in 1-butyl-3-methylimidazolium chloride/pyridine. Macromol Biosci 14(2):161–165

Engelhardt H, Orth P (1987) Alkoxy silanes for the preparation of silica based stationary phases with bonded polar functional groups. J Liq Chromatogr 10(8–9):1999–2022

Fanali C, D'Orazio G, Gentili A, Fanali S (2019) Analysis of enantiomers in products of food interest. Molecules 24(6):1119

Felix G (2001) Regioselectively modified polysaccharide derivatives as chiral stationary phases in high-performance liquid chromatography. J Chromatogr A 906(1–2):171–184

Ganske K, Heinze T (2018) Evaluation of the synthesis of soluble aromatic cellulose carbonates of low degree of substitution. Macromol Chem Phys 219(15):1800152

Harwood LA, Wong LL, Robertson J (2021) Enzymatic kinetic resolution by addition of oxygen. Angew Chem Int Ed 60(9):4434–4447

Hesse G, Hagel R (1973) Eine vollständige recemattennung durch eluitons-chromagographie an cellulose-tri-acetat. Chromatographia 6(6):277–280

Huang C, Liu J, Fang J, Jia X, Zheng Z, You S, Qin B (2022) Ketoreductase catalyzed (dynamic) kinetic resolution for biomanufacturing of chiral chemicals. Front Bioeng Biotechnol 10:929784

Ichida A, Shibata T, Okamoto I, Yuki Y, Namikoshi H, Toga Y (1984) Resolution of enantiomers by HPLC on cellulose derivatives. Chromatographia 19(1):280–284

Ikai T, Okamoto Y (2009) Structure control of polysaccharide derivatives for efficient separation of enantiomers by chromatography. Chem Rev 109(11):6077–6101

Jin L, Gao W, Li L, Ye J, Lin C, Liu W (2010) Enantioseparation and enantioselective analysis of chiral herbicides. In: Soloneski S, Laramendy M (eds) Herbicides, Theory Applications. IntechOpen, Rijeka, Croatia

Jusner P, Bausch F, Schiehser S, Schwaiger E, Potthast A, Rosenau T (2022) Protocol for characterizing the molar mass distribution and oxidized functionality profiles of aged transformer papers by gel permeation chromatography (GPC). Cellulose 29(4):2241–2256

Kaida Y, Okamoto Y (1993) Optical resolution on regioselectively carbamoylated cellulose and amylose with 3,5-dimethylphenyl and 3,5-dichlorophenyl isocyanates. Bull Chem Soc Jpn 66(8):2225–2232

Katoh Y, Tsujimoto Y, Yamamoto C, Ikai T, Kamigaito M, Okamoto Y (2011) Chiral recognition ability of cellulose derivatives bearing pyridyl and bipyridyl residues as chiral stationary phases for high-performance liquid chromatography. Polym J 43(1):84–90

Kohout M, Hovorka Å, Herciková J, Wilk M, Sysel P, Izák P, Bartůněk V, von Baeckmann C, Pícha J, Frühauf P (2019) Evaluation of silica from different vendors as the solid support of anion-exchange chiral stationary phases by means of preferential sorption and liquid chromatography. J Sep Sci 42(24):3653–3661

Lao W, Gan J (2006) High-performance liquid chromatographic separation of imidazolinone herbicide enantiomers and their methyl derivatives on polysaccharide-coated chiral stationary phases. J Chromatogr A 1117(2):184–193

Liu RQ, Bai LY, Zhang YJ, Zhang YP (2013) Green synthesis of a typical chiral stationary phase of cellulose *tris*(3,5-dimethylphenylcarbamate). Chem Cent J 7(1):1–5

Martín-Biosca Y, García-Ruiz C, Marina ML (2001) Enantiomeric separation of chiral phenoxy acid herbicides by electrokinetic chromatography. Application to the determination of analyte-selector apparent binding constants for enantiomers. Electrophoresis 22(15):3216–3225

Miaomiao H, Xiaosa J, Han Y, Xiao L, Yadong L, Shengxiang J (2017) Controlled synthesis, immobilization and chiral recognition of carboxylic acid functionalized cellulose *tris*(3,5-dimethylphenylcarbamate). Carbohydr Polym 172:223–229

Minguillón C, Franco P, Oliveros L, López P (1996) Bonded cellulose-derived high-performance liquid chromatography chiral stationary phases I. Influence of the degree of fixation on selectivity. J Chromatogr A 728(1–2):407–414

Mukherjee A, Bera A (2012) Importance of chirality and chiral chromatography in pharmaceutical industry: a detailed study. J Chem Pharm 2(4):334–346

Musa MM (2020) Enzymatic racemization of alcohols and amines: an approach for bi-enzymatic dynamic kinetic resolution. Chirality 32(2):147–157

Okada Y, Yamamoto C, Kamigaito M, Gao Y, Shen J, Okamoto Y (2016) Enantioseparation using cellulose *tris*(3,5-dimethylphenylcarbamate) as chiral stationary phase for HPLC: Influence of molecular weight of cellulose. Molecules 21(11):1484

Okamoto Y, Kaida Y (1994) Resolution by high-performance liquid chromatography using polysaccharide carbamates and benzoates as chiral stationary phases. J Chromatogr A 666(1–2):403–419

Okamoto Y, Kawashima M, Hatada K (1984) Chromatographic resolution. 7. Useful chiral packing materials for high-performance liquid chromatographic resolution of enantiomers: phenylcarbamates of polysaccharides coated on silica gel. J Am Chem Soc 106(18):5357–5359

Okamoto Y, Kawashima M, Hatada K (1986) Chromatographic resolution: XI. Controlled chiral recognition of cellulose triphenylcarbamate derivatives supported on silica gel. J Chromatogr A 363(2):173–186

Pasteur L (1858) Transformation of the two kinds of tartaric acid into racemic acid. Discovery of inactive tartaric acid. New method of separating racemic acid into the two tartaric acids, right and left. CR Acad Sci 46:615–618

Peng Y, He QS, Cai J (2016) Enantioseparation of citalopram by RP-HPLC, using sulfobutyl ether-β-cyclodextrin as a chiral mobile phase additive. Int J Anal Chem 2016:1–7

Pourjavadi A, Seidi F, Afjeh SS, Nikoseresht N, Salimi H, Nemati N (2011) Synthesis of soluble *N*-functionalized polysaccharide derivatives using phenyl carbonate precursor and their application as catalysts. Starch-Stärke 63(12):780–791

Qian D, Bera S, Hu X (2021) Chiral alkyl amine synthesis *via* catalytic enantioselective hydroalkylation of enecarbamates. J Am Chem Soc 143(4):1959–1967

Qin Q, Zhang S, Zhang WG, Zhang ZB, Xiong YJ, Guo ZY, Fan J, Run-Zheng S, Finlow D, Yin Y (2010) The impact of silica gel pore and particle sizes on HPLC column efficiency and resolution for an immobilized, cyclodextrin-based, chiral stationary phase. J Sep Sci 33(17–18):2582–2589

Rocco A, Aturki Z, Fanali S (2013) Chiral separations in food analysis. J Agric Food Chem 52:206–225

Salon MCB, Gerbaud G, Abdelmouleh M, Bruzzese C, Boufi S, Belgacem MN (2007) Studies of interactions between silane coupling agents and cellulose fibers with liquid and solid-state NMR. Magn Reson Chem 45(6):473–483

Shen J, Okamoto Y (2016) Efficient separation of enantiomers using stereoregular chiral polymers. Chem Rev 116(3):1094–1138

Shen J, Wang F, Bi W, Liu B, Liu S, Okamoto Y (2018) Synthesis of cellulose carbamates bearing regioselective substituents at 2,3- and 6-positions for efficient chromatographic enantioseparation. J Chromatogr A 1572:54–61

Singh M, Sethi S, Bhushan R (2020) Liquid chromatographic methods for separation, determination, and bioassay of enantiomers of etodolac: a review. J Sep Sci 43(1):18–30

Spelmezan CG, Bencze LC, Katona G, Irimie FD, Paizs C, Toșa ML (2020) Efficient and stable magnetic chitosan-lipase B from *Candida antarctica* bioconjugates in the enzymatic kinetic resolution of racemic heteroarylethanols. Molecules 25(2):350

Subramanian G (2008) Chiral separation techniques: a practical approach. John Wiley & Sons, Weinheim, Germany

Sun C, Li Y, Yin G (2022) Practical synthesis of chiral allylboronates by asymmetric 1,1-difunctionalization of terminal alkenes. Angew Chem Int Ed 61(37):e202209076

Tang S, Ikai T, Tsuji M, Okamoto Y (2010) Immobilization of 3,5-dimethylphenylcarbamates of cellulose and amylose onto silica gel using (3-glycidoxypropyl) triethoxysilane as linker. J Sep Sci 33(9):1255–1263

Tang S, Liu G, Li X, Jin Z, Wang F, Pan F, Okamoto Y (2011) Improved preparation of chiral stationary phases via immobilization of polysaccharide derivative-based selectors using diisocyanates. J Sep Sci 34(15):1763–1771

Wei Q, Su H, Gao D, Wang S (2019) HPLC with cellulose *tris*(3,5-dimethylphenyl carbamate) chiral stationary phase: Influence of coating times and coating amount on chiral discrimination. Chirality 31(3):164–173

Wojaczyńska E, Wojaczyński J (2020) Modern stereoselective synthesis of chiral sulfinyl compounds. Chem Rev 120(10):4578–4611

Xue YP, Cao CH, Zheng YG (2018) Enzymatic asymmetric synthesis of chiral amino acids. Chem Soc Rev 47(4):1516–1561

Yang LC, Deng H, Renata H (2022) Recent progress and developments in chemoenzymatic and biocatalytic dynamic kinetic resolution. Org. Process Res Dev 26(7):1925–1943

Yashima E, Sahavattanapong P, Okamoto Y (1996) HPLC enantioseparation on cellulose *tris*(3,5-dimethylphenylcarbamate) as a chiral stationary phase: influences of pore size of silica gel, coating amount, coating solvent, and column temperature on chiral discrimination. Chirality 8(6):446–451

Yin C, Chen W, Zhang J, Zhang M, Zhang J (2019a) A facile and efficient method to fabricate high-resolution immobilized cellulose-based chiral stationary phases *via* thiol-ene *click chemistry*. Sep Purif Technol 210:175–181

Yin C, Zhang J, Chang L, Zhang M, Yang T, Zhang X, Zhang J (2019b) Regioselectively substituted cellulose mixed esters synthesized by two-steps route to understand chiral recognition mechanism and fabricate high-performance chiral stationary phases. Anal Chim Acta 1073:90–98

Ying Z, Ling L, Kunde L, Xinping Z, Weiping L (2009) Enantiomer separation of triazole fungicides by high-performance liquid chromatography. Chirality 21(4):421–427

Yu L, Wang S, Zeng S (2019) Chiral mobile-phase additives in HPLC enantioseparations. In: Scriba GKE (ed) Chiral Separations. Springer, Humana New York, USA

Zhang GH, Xi JB, Chen W, Bai ZW (2020) Comparison in enantioseparation performance of chiral stationary phases prepared from chitosans of different sources and molecular weights. J Chromatogr A:461029

Zhang T, Francotte E (1995) Chromatographic properties of composite chiral stationary phases based on cellulose derivatives. Chirality 7(6):425–433

Zhao P, Dong X, Chen X, Guo X, Zhao L (2019) Stereoselective analysis of chiral pyrethroid insecticides tetramethrin and α-cypermethrin in fruits, vegetables, and cereals. J Agric Food Chem 67(33):9362–9370

Zheng J, Bragg W, Hou J, Lin N, Chandrasekaran S, Shamsi SA (2009) Sulfated and sulfonated polysaccharide as chiral stationary phases for capillary electrochromatography and capillary electrochromatography–mass spectrometry. J Chromatogr A 1216(5):857–872

Zhu C, Cai Y, Jiang H (2021) Recent advances for the synthesis of chiral sulfones with the sulfone moiety directly connected to the chiral center. Org Chem Front 8(19):5574–5589